Shape evolution in ^{116,118}Ru: Triaxiality and transition between the O(6) and U(5) dynamical symmetries

P.-A. Söderström,[1,*] G. Lorusso,[1] H. Watanabe,[1,2] S. Nishimura,[1] P. Doornenbal,[1] G. Thiamova,[3] F. Browne,[1,4] G. Gey,[1,3]
H. S. Jung,[5] T. Sumikama,[6] J. Taprogge,[1,7,8] Zs. Vajta,[1,9] J. Wu,[1,10] Z. Y. Xu,[11] H. Baba,[1] G. Benzoni,[12] K. Y. Chae,[13]
F. C. L. Crespi,[12,14] N. Fukuda,[1] R. Gernhäuser,[15] N. Inabe,[1] T. Isobe,[1] A. Jungclaus,[8] D. Kameda,[1] G. D. Kim,[16]
Y.-K. Kim,[16,17] I. Kojouharov,[18] F. G. Kondev,[19] T. Kubo,[1] N. Kurz,[18] Y. K. Kwon,[16] G. J. Lane,[20] Z. Li,[21] A. Montaner-Pizá,[22]
K. Moschner,[23] F. Naqvi,[24] M. Niikura,[11] H. Nishibata,[25] A. Odahara,[25] R. Orlandi,[26] Z. Patel,[27] Zs. Podolyák,[27] H. Sakurai,[1,11]
H. Schaffner,[18] G. S. Simpson,[3] K. Steiger,[15] H. Suzuki,[1] H. Takeda,[1] A. Wendt,[23] A. Yagi,[25] and K. Yoshinaga[28]

[1]*RIKEN Nishina Center, 2-1 Hirosawa, Wako-shi, Saitama 351-0198, Japan*
[2]*Department of Physics, Beihang University, Beijing 100191, China*
[3]*LPSC, Université Joseph Fourier Grenoble 1, CNRS/IN2P3, Institut National Polytechnique de Grenoble, F-38026 Grenoble Cedex, France*
[4]*School of Computing, Engineering and Mathematics, University of Brighton, Brighton BN2 4JG, United Kingdom*
[5]*Department of Physics, Chung-Ang University, Seoul 156-756, Republic of Korea*
[6]*Department of Physics, Tohoku University, Aoba, Sendai, Miyagi 980-8578, Japan*
[7]*Departamento de Física Teórica, Universidad Autónoma de Madrid, E-28049 Madrid, Spain*
[8]*Instituto de Estructura de la Materia, CSIC, E-28006 Madrid, Spain*
[9]*Institute for Nuclear Research, Hungarian Academy of Sciences, P. O. Box 51, Debrecen, H-4001, Hungary*
[10]*Department of Physics, Peking University, Beijing 100871, China*
[11]*Department of Physics, University of Tokyo, Hongo, Bunkyo-ku, Tokyo 113-0033, Japan*
[12]*INFN Sezione di Milano, I-20133 Milano, Italy*
[13]*Department of Physics, Sungkyunkwan University, Suwon 440-746, Republic of Korea*
[14]*Dipartimento di Fisica, Università di Milano, I-20133 Milano, Italy*
[15]*Physik Department E12, Technische Universität München, D-85748 Garching, Germany*
[16]*Rare Isotope Science Project, Institute for Basic Science, Daejeon 305-811, Republic of Korea*
[17]*Department of Nuclear Engineering, Hanyang University, Seoul 133-791, Republic of Korea*
[18]*GSI Helmholtzzentrum für Schwerionenforschung GmbH, 64291 Darmstadt, Germany*
[19]*Nuclear Engineering Division, Argonne National Laboratory, Argonne, Illinois 60439, USA*
[20]*Department of Nuclear Physics, R.S.P.E., Australian National University, Canberra, A.C.T. 0200, Australia*
[21]*School of Physics, Peking University, Beijing 100871, China*
[22]*Instituto de Física Corpuscular, CSIC-University of Valencia, E-46980 Paterna, Spain*
[23]*Institut für Kernphysik, Universität zu Köln, Zülpicher Strasse 77, D-50937 Köln, Germany*
[24]*Wright Nuclear Structure Laboratory, Yale University, New Haven, Connecticut 06520-8120, USA*
[25]*Department of Physics, Osaka University, Machikaneyama-machi 1-1, Toyonaka, Osaka 560-0043, Japan*
[26]*Instituut voor Kern en Stralingsfysica, KU Leuven, University of Leuven, B-3001 Leuven, Belgium*
[27]*Department of Physics, University of Surrey, Guildford GU2 7XH, United Kingdom*
[28]*Department of Physics, Tokyo University of Science, 2641 Yamazaki, Noda, Chiba 278-8510, Japan*

^{116}Ru and ^{118}Ru have been studied via β-delayed γ-ray spectroscopy of nuclei produced in fragmentation reactions at the Radioactive Ion-Beam Factory (RIBF) facility. Level schemes with positive-parity states up to spin $J = 6$ have been constructed. The results have been discussed in terms of the interacting boson model, the algebraic collective model, and total Routhian surfaces. We conclude that the very neutron-rich nuclei still show many features associated with triaxial γ-soft nuclei, represented by the O(6) symmetry, but are approaching a spherical structure, the U(5) symmetry, with increasing neutron number towards the $N = 82$ shell closure. In ^{118}Ru, hints of a shape transition in the ground state have been observed.

I. INTRODUCTION

One of the central features in our understanding of the atomic nucleus is the appearance of magic numbers. Isotopes in their proximity can be described in terms of single-particle interactions with an inert core. Most nuclei, however, lie sufficiently far from magic numbers for collective behavior to dominate over the single-particle structure. This quadrupole collectivity gives rise to a variety of nuclear shapes and excitations. In the prolate-oblate transition regions comparable energy minima of the shapes can lead to shape coexistence. The prolate-oblate shape interaction produces a potential in which axially asymmetric vibrations are prevalent. In such a γ-soft potential even stable intermediate shapes without any symmetry axis, so called triaxial nuclei, can exist.

_____

[*]pasoder@ribf.riken.jp

The neutron-rich nuclei in the $28 < Z < 50$ region are interesting systems for studying the evolution of collectivity. They lie far enough away from closed shells for well established deformations to evolve, but close enough to shell closures for microscopic excitations to compete with collectivity. This can, for example, be seen in the recent experimental results presented in Ref. [1] where subshell gaps at $N = 64$ and $N = 70$ were discussed for zirconium isotopes.

Shape evolution in neutron-rich ruthenium isotopes up to ^{114}Ru has been studied with γ-ray spectroscopy [2–5]. Both ^{116}Ru and ^{118}Ru, have been produced previously by fission of ^{238}U [6] and fragmentation of ^{136}Xe [7], but no information on excited states in these nuclei has been obtained to date. Theoretical work on ruthenium isotopes has suggested a well established triaxial shape for the $^{100-110}$Ru isotopes, while ^{112,114}Ru would have a γ-soft nature. The triaxial shape is predicted to reappear for ^{116}Ru and gradually fade away when approaching the $N = 82$ shell closure [8,9].

The region of the nuclear chart discussed in this paper is a good testing ground for the interacting boson model (IBM), as many features of the nuclei can be well described while providing challenges for the model through the triaxial nature in many of these nuclei. Thus, much theoretical attention has been paid to this region [10–14]. The new data obtained in this experiment can be valuable to further develop our understanding of the role of dynamical symmetries in atomic nuclei.

Results from a β-delayed γ-ray spectroscopy experiment on ^{116}Ru and ^{118}Ru, performed at RIKEN Nishina Center, are presented. The results are discussed in terms of energy systematics, the IBM, the algebraic collective model (ACM), and total Routhian surfaces (TRS).

II. EXPERIMENT

The experiment was carried out using the accelerator complex and magnetic spectrometers at the Radioactive Ion-Beam Factory (RIBF) of the RIKEN Nishina Center. The accelerator chain up to the superconducting ring cyclotron [15] was used to accelerate a ^{238}U beam to an energy of 345 MeV/u with average intensity of $\sim$10 p nA. The uranium beam impinged on a 555 mg/cm^2 beryllium target, inducing fission of the uranium beam. After the target, the BigRIPS separator [16] was used for separation and tagging of the

exotic nuclei of interest. The ZeroDegree spectrometer [17] provided A/q and Z on an event-by-event basis through the magnetic rigidity, time-of-flight, and energy loss of the ions ($B\rho$–TOF–ΔE). The particle identification analysis was carried out using measurements $B\rho$ in parallel-plate avalanche counter detectors at F3, F5, and F7; the TOF between plastic scintillators placed at F5 and F7; and the ΔE in an ionization chamber placed at F11.

The secondary beam was implanted into a stack of double-sided silicon strip detectors (DSSSDs). The β-delayed γ rays were detected within the Euroball-RIKEN Cluster Array (EURICA) [18–21] high-purity germanium (HPGe) detector array. The DSSSD stack used was WAS3ABi (wide-range active silicon strip stopper array for β and ion detection). Each DSSSD in the WAS3ABi array comprises 40×60 strips of 1 mm thickness. WAS3ABi is further described in Ref. [19,21]. The implantation rate in WAS3ABi was $\sim$50 particles per second. In total, $\sim$2.6 · 10^5 ^{116}Tc and $\sim$1.3 · 10^4 ^{118}Tc nuclei were implanted during the experiment. The efficiency to detect β decays in WAS3ABi was $\sim$40%.

The EURICA array consisted of twelve Euroball IV HPGe cluster detectors [22–24], each built from seven tapered, hexaconical HPGe crystals in a close-packed configuration. The clusters were arranged in three rings at 51° (five clusters), 90° (two clusters), and 129° (five clusters) relative to the beam axis. The nominal distance from the front face of the clusters to the center is 22 cm; however, in this experiment the clusters had been moved closer to the WAS3ABi chamber, when possible, to increase the efficiency.

III. RESULTS

The β-delayed γ-ray spectra associated with ^{116}Tc and ^{118}Tc are shown in Figs. 1 and 2, respectively. Contributions from the β-decay granddaughters ^{116}Rh and ^{118}Rh were suppressed by setting a time condition in WAS3ABi so that only β-decay events within 100 ms following implantation in the same or an adjacent pixel were accepted. This approximately corresponds to twice the half-life of the Tc isotopes, and was thus long enough to include most of the decays into the nuclei of interest. At the same time, the half-lives of ^{116}Ru and ^{118}Ru have been measured previously to be 204 and 123 ms, respectively, [7] which means that their decays
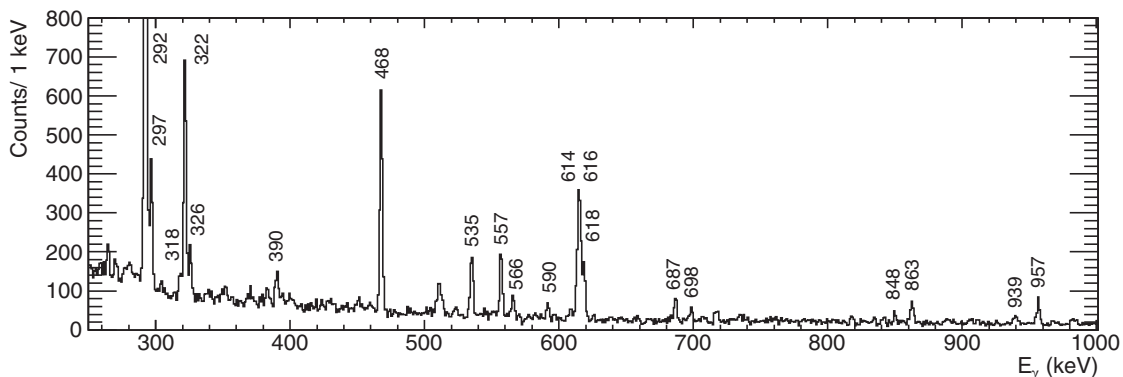

FIG. 1. Spectrum of γ rays following the β decay of ^{116}Tc. Transitions from excited states in ^{116}Ru, from this work, have been labeled. The height of the 292 keV γ-ray peak is $\sim$2100 counts.
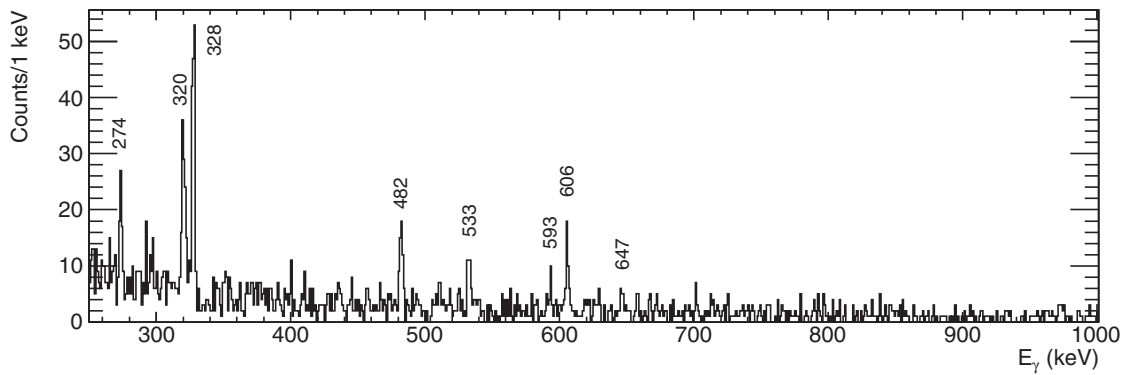
FIG. 2. Spectrum of γ rays following the β-decay of ^{118}Tc. Transitions from excited states in ^{118}Ru, from this work, have been labeled.

are mostly outside the time gate. This method can not suppress the contribution from ^{115}Ru and ^{117}Ru, following β-delayed neutron emission. This is estimated to be 20%–25% of the β decays [25] and would primarily result in low-energy γ rays.

The relations between the different γ rays observed has been studied using the $\gamma\gamma$-coincidence technique and, for ^{116}Ru, verified using $\gamma\gamma\gamma$ coincidences. The strongest γ rays seen in the singles spectra, 292 and 328 keV for ^{116}Ru and ^{118}Ru, respectively, have been assigned to the decay of the first excited 2^+ states. The second and third strongest transitions, 322 and 468 keV for ^{116}Ru, and 320 and 482 keV for ^{118}Ru, were assigned to the 2_2^+ and 4_1^+ states, respectively. For ^{118}Ru, the $2_2^+ \rightarrow 0_1^+$ transitions has been tentatively assigned as the 647 keV γ ray, corresponding to the sum of the 328 and 320 keV transitions. It can be seen in the singles spectrum, but the statistics are too low to clearly separate the peak from the background in $\gamma\gamma$ coincidences. Similarly, the 616 and 606 keV γ-rays for ^{116}Ru and ^{118}Ru, respectively, were assigned to the 6_1^+ states.

In coincidence with the $2_2^+ \rightarrow 2_1^+$ transitions are γ rays of 535 keV for ^{116}Ru and 533 keV for ^{118}Ru. These γ rays have been interpreted as originating from the 4_2^+ states in their respective nuclei. Further strengthening this assignment, in ^{116}Ru is a weak transition of 390 keV observed in coincidence

that would correspond to the $4_2^+ \rightarrow 4_1^+$ transition. Again, the 390 keV transition is tentative, as a weak transition, believed to originate from the 5_2^+ state with the same energy is observed in coincidence with other γ rays.

Using similar arguments as for the 2_2^+ and 4_2^+ states in ^{116}Ru, three observed γ-ray transitions of 297, 557, and 619 keV can be assigned to the odd-parity quasi-γ levels with spin and parity 3_1^+ and 5_1^+. For ^{118}Ru, two corresponding γ-ray transitions with the energies 274 and 593 keV were observed. For ^{116}Ru, a weak 318 keV γ ray, not seen in the $\gamma\gamma$ coincidences, has been tentatively assigned to the $5_1^+ \rightarrow 4_2^+$ transition. A γ ray with an energy of 687 keV, also observed in coincidence with the 535 keV transition, was assigned to the 6_2^+ state.

Besides the transitions mentioned above, several other γ rays were observed in $\gamma\gamma$ and $\gamma\gamma\gamma$ coincidences, but could not be unambiguously assigned to states with specific spin and parity. It is worth noting that these γ rays give rise to a quadruplet of states which are very similar to the quadruplet of 4^+ states obtained from the IBM. However, as this similarity could be coincidental, we do not consider this argument strong enough for an assignment of these levels to the 4_{4-7}^+ states. The level schemes resulting from this analysis are shown in Figs. 3 and 4. Tables I and II summarize these results.
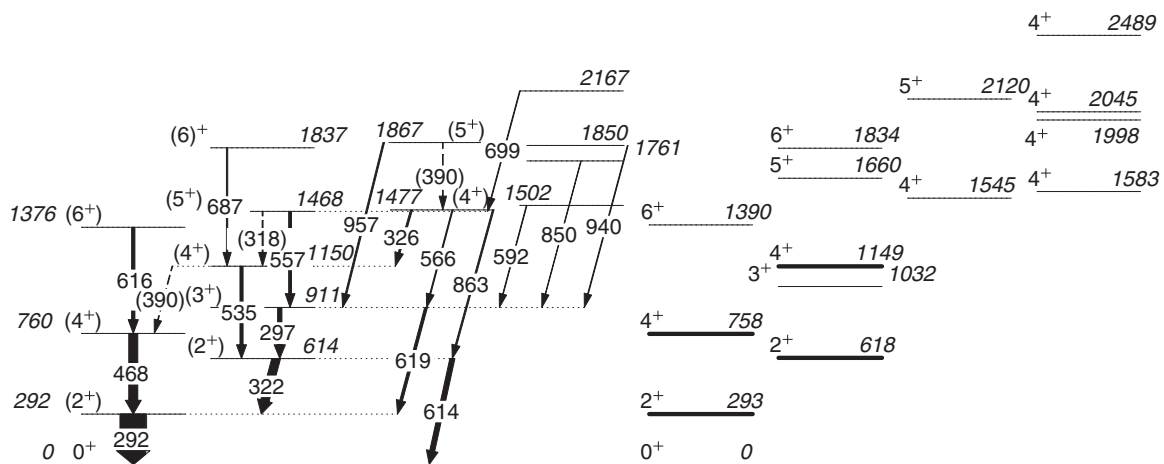

FIG. 3. Experimental level scheme of ^{116}Ru as obtained in this work (left) and calculated from the IBM-1 model (right). The thicknesses of the arrows are proportional to the intensities of the γ rays. The thick levels in the IBM-1 level scheme have been used to fit the energies of the model to the experimental data.
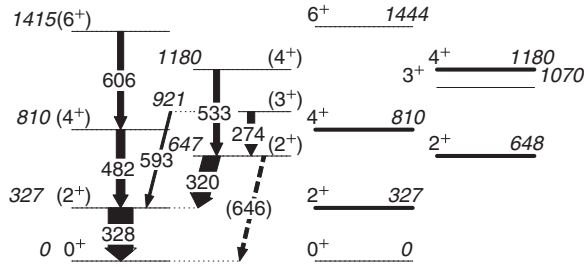
FIG. 4. Experimental level scheme of ^{118}Ru as obtained in this work (left) and calculated using the IBM-1 model (right). The thick levels in the IBM-1 level scheme have been used to fit the energies of the model to the experimental data.

A search for excited 0^+ states has also been carried out, by selecting events corresponding to two β decays from the grandmothers $^{112-116}$Mo. As the even-even Mo isotopes should have 0^+ ground states, their β decays are expected to mainly populate low-spin states in $^{112-116}$Tc. If these low-spin states undergo β decay, it is expected that low-spin states in $^{112-116}$Ru would be favored. Indeed, the γ rays seen in the resulting spectra were mainly associated with the 2^+ and 3^+ states. However, no additional γ rays that could be associated with a $0_2^+ \rightarrow 2_1^+$ decay were observed.

A log ft analysis of the states in ^{116}Ru gives surprisingly similar values of approximately 5.8(5). Thus, it was not possible to unambiguously assign the spin and parity of

TABLE I. Initial level energy E_i and spin-parity J_i^π of the levels obtained for ^{116}Ru in this work. For each γ ray the energy E_γ, γ-ray branching ratio B_γ, singles intensity I_γ, final level energy E_f, and final level spin J_f^π, are listed. A systematic uncertainty of 0.25 keV has been added to the statistical uncertainty in E_γ. Similarly, a systematic uncertainty of 10% was added to I_γ.

E_i (keV)	J_i^π	E_γ (keV)	B_γ	I_γ	E_f (keV)	J_f^π
292.43(35)	(2^+)	292.43(25)	100	100(10)	0	0^+
614.3(4)	(2^+)	321.76(25)	100(16)	32(4)	292	(2^+)
		614.29(33)	59(11)	19.2(27)	0	0^+
760.1(5)	(4^+)	467.68(25)	100	35(4)	292	(2^+)
910.8(4)	(3^+)	296.65(26)	100(18)	16.3(21)	614	(2^+)
		618.57(27)	64(13)	10.4(17)	292	(2^+)
1150.0(5)	(4^+)	389.8(5)	22(16)	2.6(18)	760	(4^+)
		535.17(26)	100(20)	11.9(17)	614	(2^+)
1375.7(7)	(6^+)	615.59(25)	100	13.6(20)	760	(4^+)
1468.0(5)	(5^+)	318.14(32)	32(10)	3.4(10)	1150	(4^+)
		557.04(25)	100(21)	10.9(16)	911	(3^+)
1476.5(5)	(4^+)	325.73(27)	100(27)	6.9(13)	1150	(4^+)
		565.82(29)	57(18)	3.9(10)	911	(3^+)
		862.66(29)	81(23)	5.6(11)	614	(2^+)
1502.5(7)		591.63(31)	100	2.5(7)	911	(3^+)
1760.7(7)		849.81(30)	100	1.9(9)	911	(3^+)
1836.7(7)	(6^+)	686.66(28)	100	4.9(10)	1150	(4^+)
1850.3(8)		939.50(42)	100	2.8(9)	911	(3^+)
1867.1(6)	(5^+)	390.04(39)	37(25)	2.1(14)	1477	(4^+)
		956.57(28)	100(31)	5.8(13)	911	(3^+)
2166.5(8)		698.50(36)	100	2.6(11)	1468	(5^+)

TABLE II. Same as Table I for ^{118}Ru.

E_i (keV)	J_i^π	E_γ (keV)	B_γ	I_γ	E_f (keV)	J_f^π
327.3(5)	(2^+)	327.64(25)	100	100(10)	0	0^+
647.3(5)	(2^+)	320.24(25)	100(16)	68(7)	327	(2^+)
		646.5(4)	22(9)	15(6)	0	0^+
809.6(6)	(4^+)	482.27(26)	100	35(4)	327	(2^+)
920.7(6)	(3^+)	273.50(32)	100(50)	29(9)	648	(2^+)
		593.35(29)	34(15)	9.9(28)	327	(2^+)
1180.0(7)	(4^+)	532.75(28)	100	25(4)	648	(2^+)
1415.3(8)	(6^+)	605.68(26)	100	25(5)	1181	(4^+)

^{116}Tc. The similar log ft values could be explained by a low-spin (high-spin) ground state and a high-spin (low-spin) β-decaying isomer. In that case, the isomer should have a lifetime similar to the ground state. This would imply that when β-decay events are selected, both decays from the ground state and isomeric state are seen in the γ-ray spectra. However, as stated previously, when gating on the ^{116}Mo nucleus only γ rays from low-spin states are seen in the spectrum. If the ground (isomeric) state in ^{116}Tc has $J \leqslant 3$ and the isomeric (ground) state has $J \geqslant 4$, this could give the even log ft distribution observed in the data. This would be consistent with previous measurements of ^{114}Tc decaying into ^{114}Ru [26] where two states with $J^P = (1^+)$ and $J \geqslant (4)$ produce a similar log ft pattern as observed for the decay of ^{116}Tc. Assuming an oblate deformation similar to [26], the main orbitals that contribute to the ground states of ^{116,118}Tc should be $\pi 5/2[422] \otimes \nu 5/2[532]$ and $\pi 5/2[422] \otimes \nu 3/2[541]$, respectively. This means that ^{116}Tc should have a spin-parity of either 0^- or 5^- in the ground state, and ^{118}Tc should have either 1^- or 4–6^-. It is worth stressing that this interpretation is only tentative due to the possible presence of a "pandemonium" effect [27]. The high Q_β value of ~ 12 MeV for ^{116}Tc could in fact cause a large number of high-energy excited states to fragment the γ-ray distribution.

The kinematic moment of inertia, $\mathcal{J}^{(1)} = \tilde{I}/\omega$, has been calculated for the ground-state bands and the quasi-γ bands of $^{114-118}$Ru. We have used the point-difference approximation for these calculations,

$$\omega = \frac{dE}{d\tilde{I}} \approx \frac{\Delta E}{\Delta \tilde{I}}, \quad (1)$$

where $\tilde{I} = \sqrt{J(J+1) - K^2}$, J being the spin of the level and K being the spin of the band head. As seen in Fig. 5, $\mathcal{J}^{(1)}$ for the levels in $^{116-118}$Ru are consistent with $\mathcal{J}^{(1)}$ for the corresponding levels in ^{114}Ru. This strengthen the assignments for the ground-state and quasi-γ bands in this work.

IV. DISCUSSION

The energy ratio $R(4/2) = E(4_1^+)/E(2_1^+)$ is a well known observable of the extent of quadrupole deformation, having the minimum at $R(4/2) = 2$ for spherical nuclei and the maximum $R(4/2) = 3.33$ for rigid rotors. The trends of this ratio as a function of N for Mo, Ru, and Pd chains, shown in Fig. 6, indicate that these elements are well deformed in this region. The Pd chain having a relatively stable value around the
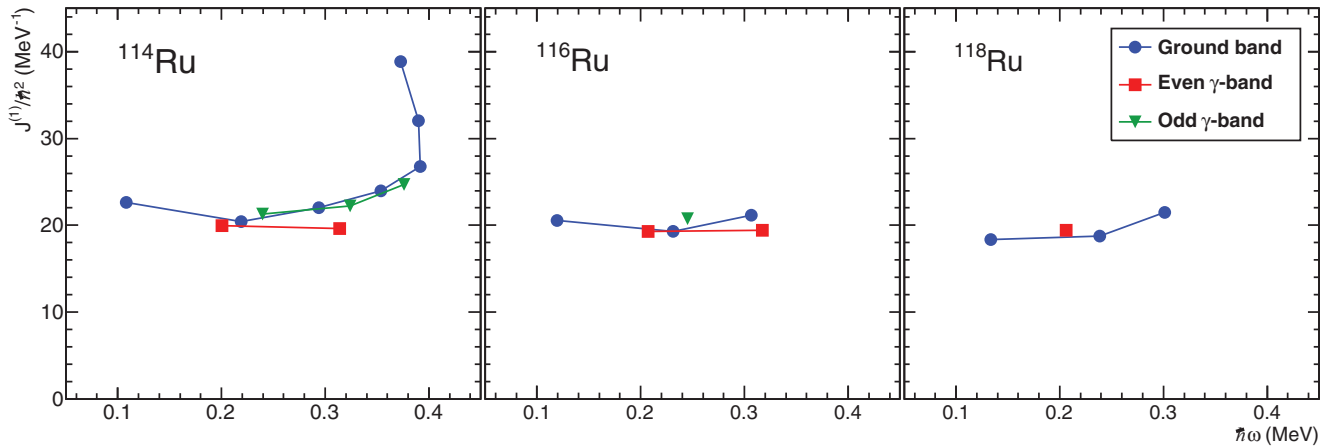
FIG. 5. (Color online) Kinematic moment-of-inertia $\mathcal{J}^{(1)}$ as a function of the rotational frequency $\hbar\omega$ for the ground-state and quasi-γ bands in $^{114-118}$Ru.

transitional limit, $R(4/2) = 2.5$, while the Mo chain is closer to the deformed limit and the Ru chain lies in between these two. For the most neutron-rich Ru isotopes, studied in this experiment, the beginning of the transition towards sphericity can clearly be seen.

The degree of axial asymmetry in collective nuclei is strongly associated with the energy of the bandhead in the quasi-γ band $E(2_2^+)$; this is accentuated when compared to the energy of the $E(4_1^+)$ state. By defining $E_s = E(2_2^+) - E(4_1^+)$ and studying the ratio $E_s/E(2_1^+)$ [29], shown in Fig. 7, the evolution of axial asymmetry is obvious. The trends for all three Mo, Ru, and Pd chains are similarly decreasing, reaching a minimum of $E_s/E(2_1^+) \approx -0.5$ at neutron number $N = 68$, while stabilizing about this value for $N > 68$. In Ref. [29] an interesting discussion was presented, comparing these nuclei to corresponding isotopes in the $A \approx 190$ region. In this heavier region the behavior of the W, Os, and Pt chains shows a remarkable similarity with the Mo, Ru, and Pd chains, respectively. One interesting discrepancy, however, is the sudden increase of $E_s/E(2_1^+)$ for ^{194}Os that is not present in ^{114}Ru. This has been interpreted as a shape transition into oblate shape for the Os chain [30]. However, no such increase

is observed in either ^{116}Ru nor ^{118}Ru, implying that the triaxial nature of these nuclei persists.

A. Cranked shell model

TRS calculations have also been carried out for the $^{114-120}$Ru isotopes. This model treats all the nucleons equivalently as particles moving in a rotating mean field and makes no distinction between core and valence particles. In this model, the total energy of an n-quasiparticle configuration is given by the contribution from the macroscopic as well as the microscopic properties of the nucleus. The macroscopic part was taken from the liquid drop model, where the pairing energy is calculated using the Lipkin-Nogami method [31]. The Strutinsky shell correction [32,33] method is applied to obtain the microscopic total energy. When the system is defined, it is rotated by a frequency $\hbar\omega$, after which the effects on the single-particle orbitals in the rotating potential are calculated. For details about the code used in the TRS calculations, see Refs. [34–36]. The calculations have been
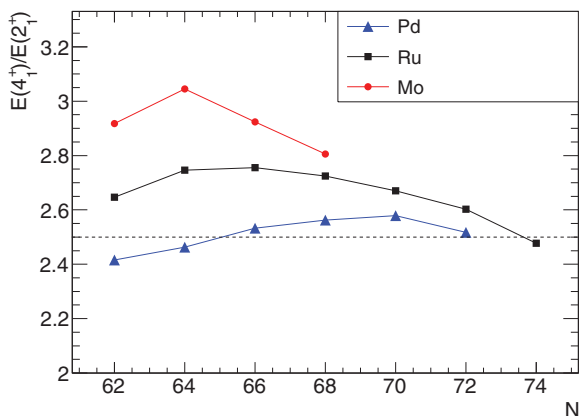

FIG. 6. (Color online) Experimental energy ratio between the 4_1^+ and 2_1^+ states, $R(4/2)$, for the neutron-rich molybdenum, ruthenium, and palladium isotopes from [28] and this work.
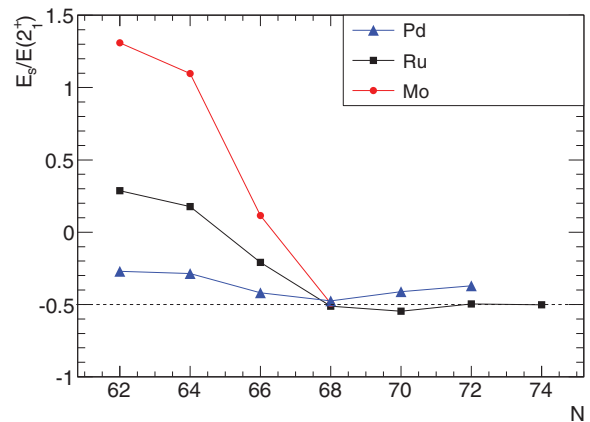

FIG. 7. (Color online) Experimental ratio of the difference between the 2_2^+ and 4_1^+ states, and the energy of the 2_1^+ state, $E_s/E(2_1^+)$, for the neutron-rich the molybdenum, ruthenium, and palladium isotopes.
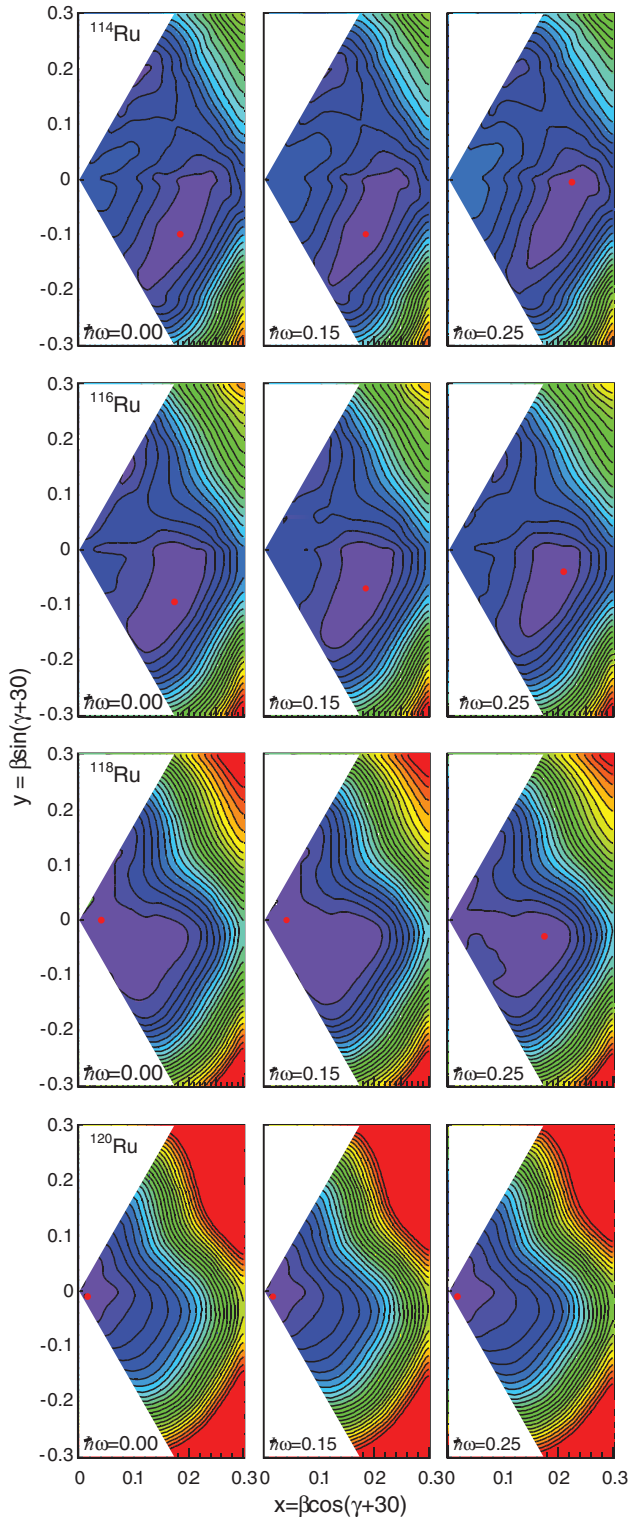
FIG. 8. (Color online) Total Routhian surface calculations for the even-even nuclei $^{114-120}$Ru. The calculations have been performed for rotational frequencies $\hbar\omega = 0.00$, $\hbar\omega = 0.15$, and $\hbar\omega = 0.25$, approximately corresponding to the 0^+_1, 2^+_1, and 4^+_1 states, respectively. The Routhian minima are shown with a red circle in each surface. Each contour line is separated by 200 keV.

TABLE III. Locations of the Routhian minima in the (β, γ) plane, for the calculations in Fig. 8.

Isotope	$\hbar\omega = 0.00$		$\hbar\omega = 0.15$		$\hbar\omega = 0.25$	
	β	γ	β	γ	β	γ
^{114}Ru	0.21	−58	0.21	−58	0.21	−31
^{116}Ru	0.20	−58	0.20	−51	0.21	−41
^{118}Ru	0.04	−30	0.04	−30	0.18	−40
^{120}Ru	0.02	−64	0.02	−64	0.02	−64

performed at the rotational frequencies $\hbar\omega = 0.00$, 0.15, and 0.25, roughly corresponding to the spins of the 0^+_1, 2^+_1, and 4^+_1 states, respectively. The results of these calculations are shown in Fig. 8 and Table III. Even this simple approach using standard input parameters gives results similar to the recent detailed studies by Möller *et al.* [8,9].

The TRS calculation gives a γ-soft triaxial minimum around $\gamma = -60°$ that does not change over the range of rotational frequencies used for calculations, both for ^{114}Ru and ^{116}Ru. The values $\gamma = 30$ and $\gamma = -60°$ correspond to prolate and oblate triaxial minima, respectively. However, since no direct measurement of the deformation was done in this experiment, both types of deformation were considered in the discussion. For ^{120}Ru, the TRS calculations give a very pronounced spherical minimum that is stable over the rotational frequency range. A noteworthy point in these calculations is a spherical minimum in ^{118}Ru, which drastically changes its shape at $\hbar\omega = 0.25$. Such a shape transition could make ^{118}Ru look more deformed in the IBM-1 model than it actually is in its ground state because the $R(4/2)$ value, that determines the ζ parameter, would be associated with the deformed 4^+_1 state. However, even if the transition probability that determines the χ parameter would be associated with a more spherical nature of the 2^+_2 state, both the U(5) and O(6) limits exhibit the same $E2$ transition probabilities, and a largely unaffected χ parameter [37]. It is not possible to draw any definite conclusions about this issue without a direct measurement of the ground-state deformation, but if this shape change occurs it should push ^{118}Ru even more into the U(5) region.

B. Interacting boson model

The IBM is a truncation of the shell model that uses the nucleon pairing interaction as a starting point and couples pairs of nucleons as bosons. In the IBM-1 it is assumed that only monopole (s) and quadrupole (d) bosons with $J^P = 0^+$ and $J^P = 2^+$, respectively, contribute to the excited configurations. By requiring that the IBM operators are properly normalized they will satisfy the commutation relations of the algebraic U(6) group. To make the angular momentum a good quantum number, the rotational group O(3) has to be included in the symmetry reduction chain. The main differences that arise from this reduction in subgroups are the U(5) symmetry, corresponding to a spherical vibrating nucleus, and the O(6) symmetry, corresponding to a γ-soft nucleus.

A simplified way to write a Hamiltonian that contains these chains of subgroups is

$$\frac{\hat{\mathcal{H}}}{c} = (1 - \zeta)\hat{n}_d + \frac{\zeta}{4N_B}\hat{Q}^\chi \cdot \hat{Q}^\chi + 2\lambda\hat{L}\cdot\hat{L}, \qquad (2)$$

with the quadrupole operator

$$\hat{Q}^\chi = [d^\dagger \times s + s^\dagger \times d]^{(2)} + \chi[d^\dagger \times d]^{(2)}. \qquad (3)$$

The above equations consist of the d-boson number operator $\hat{n}_d$, the angular momentum operator $\hat{L}$, and the s- (d-) boson creation and destruction operators s and $s^\dagger$ (d and $d^\dagger$), respectively. The relative strengths of these operators are determined by the parameters ζ, N_B, λ, and χ, while c determines the absolute normalization of the energy eigenstates. Here N_B is the number of valence bosons in the calculations.

In order to fit the IBM-1 Hamiltonian to experimental data we need information that is sensitive to the known observables. The $\hat{n}_d$ operator is strongly correlated with the energy ratio of the 4_1^+ and the 2_1^+ states, $R(4/2)$. The $\hat{L}$ operator is related to the lowering of the 2_2^+ state with respect to the 4_1^+ state. Normally, the χ parameter would be determined from the energy gap between the 2_2^+ and the 0_2^+ states. However, as experimental information of the 0_2^+ states is not available in the nuclei under investigation, we have instead used the quadrupole transition probability,

$$\hat{T}(E2) = e_B\hat{Q}^\chi. \qquad (4)$$

Using the consistent-Q formalism [38], the parameter χ of $\hat{Q}^\chi$ in (2) and (4) will have the same value. The e_B parameter is the effective boson charge that gives absolute normalization of the $B(E2)$ values, but by using the transition strength ratio between the $2_2^+ \rightarrow 0_1^+$ and the $2_2^+ \rightarrow 2_1^+$ transitions we will have an observable that is sensitive to χ, while being independent of e_B.

We now have a Hamiltonian that can be completely fitted to experimental observables, and that can be used to interpret most of the excited states obtained in the experiment. The only exception to this is the signature splitting between even-spin states and odd-spin states in the γ band. This is because this signature splitting is related to the triaxiality of the nucleus, while the simplest IBM-1 Hamiltonian does not give any triaxial minima. It has been shown that adding a cubic term to the IBM Hamiltonian, corresponding to triaxial deformation, will wash out the odd-even staggering in the quasi-γ bands and give the evenly spaced level structure seen in the experimental data [14].

IBM-1 calculations have been carried out for the even-even $^{108-118}$Ru isotopes using the PHINT and FBEM codes [39] and the parameters listed in Table IV. It has been observed that, within a chain of isotopes, good agreement can be obtained keeping $c\lambda$ approximately constant [40]. Thus, this quantity was fitted globally for all the isotopes, while the other parameters were fitted individually. The path of the neutron-rich Ru isotopes in the Casten triangle [38] is shown in Fig. 9.

These calculations give a good agreement with experimental data for all of the nuclei that were fitted; see examples in Figs. 3 and 4 and Table V. As expected, a smooth transition from the vicinity of the O(6) limit towards the U(5) limit is observed.

TABLE IV. Parameters used for the IBM-1 calculations that best reproduce the low-energy spectra using the IBM-1 Hamiltonian in (2), for the even-even neutron-rich ruthenium isotopes.

Isotope	c	ζ	χ	$c\lambda$	N_B
^{108}Ru	1.579	0.814	-0.235	0.0068	10
^{110}Ru	1.082	0.669	-0.429	0.0068	11
^{112}Ru	0.827	0.617	-0.390	0.0068	10
^{114}Ru	0.816	0.568	-0.368	0.0068	9
^{116}Ru	0.770	0.503	-0.435	0.0068	8
^{118}Ru	0.641	0.402	-0.469	0.0068	7

The results of these calculations have also been compared to a recently published work where the IBM parameters have been calculated using mean-field methods, and excited states for neutron-rich Ru isotopes have been predicted [11]; see Fig. 10. Furthermore, Ref. [11] uses the IBM-2 model with separate proton and neutron degrees of freedom. The IBM-2 model is well suited for those kind of predictions as it gives a stronger microscopic foundation based on the spherical model to the IBM [41,42]. The mean-field approach does reproduce the data well for the isotopes with, at the time of that work, known excited states, except for the 2_2^+ state where the energies are systematically overestimated. However, the new data presented in this paper show a clear deviation from the predicted systematics of the yrast band. The IBM-2 model with mean-field parameters do reproduce the experimental data for $N = 64$, but deviates at $N = 66$. Note that these calculations, although having more parameters, have their parameters fixed from mean-field calculations. They are, thus, not fitted to the experimental data. In the IBM-1 fits, the absolute value of the 0_2^+ energy in ^{108}Ru is well reproduced. For states with $N \geqslant 66$ the IBM-1 and IBM-2 calculations diverge, the IBM-1 giving a sharp decrease in energies and the IBM-2 a smooth increase that follows the systematics of the yrast band and the 2_2^+
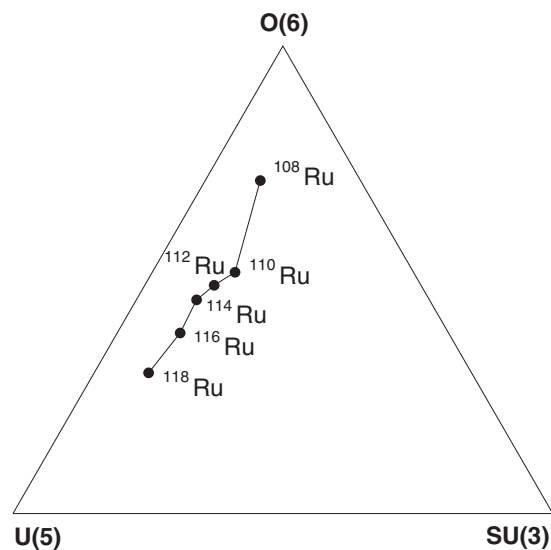

FIG. 9. Trajectory of the neutron-rich ruthenium isotopes in the Casten triangle, as obtained by fitting the IBM-1 Hamiltonian in Eq. (2) to experimental data.

TABLE V. Experimental values and IBM-1 calculated values for the observables used to evaluate the IBM-1 parameters for the most neutron-rich nuclei, as well as for a pure configuration of the three dynamical symmetries with $N_B = 10$. Note that a value of $\lambda = 0$ has been used for the pure symmetry limits, which gives an overestimation of the $R(2_2^+/2_1^+)$ values, with respect to the experimental data.

Ratio	^{114}Ru		^{116}Ru		^{118}Ru		U(5)	O(6)	SU(3)
	Expt.	IBM	Expt.	IBM	Expt.	IBM			
$R(4_1^+/2_1^+)$	2.6705(21)	2.6644	2.599(4)	2.5901	2.474(4)	2.473	2.00	2.50	3.33
$R(2_2^+/2_1^+)$	2.1242(19)	2.1373	2.1007(28)	2.1145	1.978(4)	1.978	2.00	2.50	28.8
$R((4_2^+ - 2_2^+)/2_1^+)$	1.9555(24)	1.9118	1.8321(30)	1.8114	1.625(7)	1.627	1	2	2.29
$\frac{2_2^+ \to 0_1^+}{2_2^+ \to 2_1^+}$	2.7(7)	3.7	2.3(4)	1.5	0.36(26)	0.67	0	0	136
$\frac{4_2^+ \to 4_1^+}{4_2^+ \to 2_2^+}$	120(90)	70	110(80)	70	170(110)	80	91	91	0

state. This behavior of the 0_2^+ states cannot be explained with current data, but several subtle effects could influence the 0_2^+ systematics. For example, shape coexistence and interactions between the 0_1^+, 0_2^+, and possibly also the 0_3^+ states could play a significant role. For recent discussion about the 0^+ states in lighter Ru isotopes, see Ref. [43].
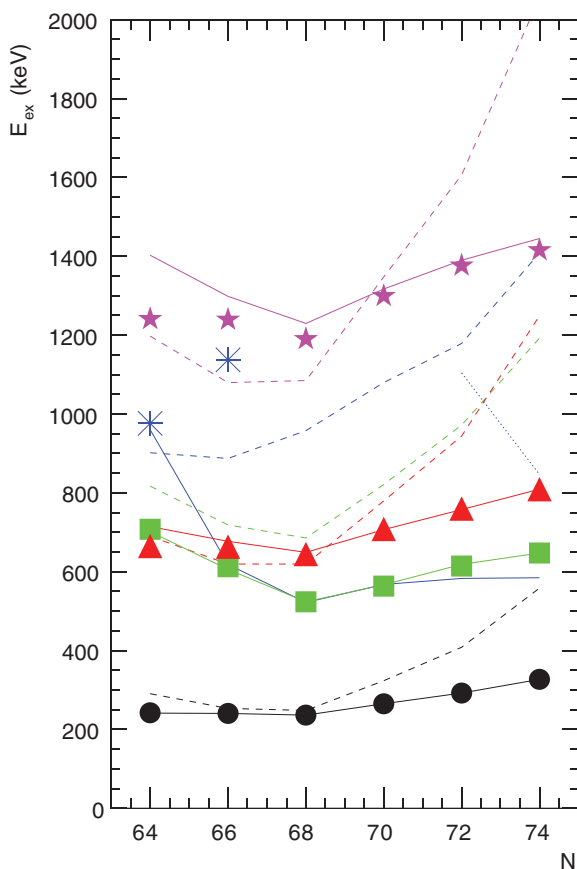

FIG. 10. (Color online) Experimental (symbols) and calculated (lines) energy systematics of the 2_1^+ (black circles), 2_2^+ (green squares), 4_1^+ (red triangles), 0_2^+ (blue asterisks), and 6_1^+ (magenta stars) in the Ru isotopes. The solid lines show the IBM-1 fits from this work, while the dashed lines show the IBM-2 calculation from Ref. [11]. Algebraic collective model calculations of the 0_2^+ states for $N = 72, 74$, see Sec. IV C, are shown as a dashed line.

C. Algebraic collective model

One recent approach to describing collective phenomena in nuclei is the development of the algebraic collective model (ACM) [44]. By formulating the Bohr model of collective nuclei in terms of Lie algebra, both the simplicity of the IBM and the phenomenological properties of the Bohr model can be obtained simultaneously. In principle, the radial part of the wave functions, as described by the β parameter, can be separated from the angular part of the wave functions, described by the γ parameter and a triple Ω of Euler angles, that describes SO(3) rotation. Using techniques from group theory, calculations can be performed in the (β, γ, Ω) coordinate system. Recent work on this model has shown the close relation between the Bohr model, the ACM, and the IBM in the triaxial limit [45].

The ACM Hamiltonian used in the current work was

$$\hat{\mathcal{H}} = -\frac{\nabla^2}{2M} + \frac{1}{2}M[(1 - 2\alpha)\beta^2 + \alpha\beta^4] - \chi_A \beta \cos 3\gamma + \kappa_A \cos^2 3\gamma, \quad (5)$$

where the mass parameter M determines the depth of the energy minimum and α determines the shape of the radial potential. Typically, these two parameters are in the ranges $10 \leqslant M \leqslant 100$ and $0 \leqslant \alpha \leqslant 2$ [44]. For $\alpha < 0.5$, the potential will have a spherical minimum and for larger values of α the nucleus becomes prolate deformed. The angular part of the Hamiltonian has two components, the linear term gives an axially symmetric energy minimum at $\gamma = 0°$ and the quadratic term gives a triaxial energy minimum at $\gamma = 30°$. By adjusting the χ_A and κ_A parameters any amount of triaxial deformation between these two limits can be obtained.

In Fig. 11, the excitation energy spectra from the ACM calculations are compared with experimental data. Overall, the calculations reproduce the experimental data well, even if some deviations can be seen. The reason for these deviations is the relatively small value of M and a negligible value of χ_A giving a soft potential in both the β and γ directions, which induces a significant centrifugal stretching, and the interaction of γ and rotational degrees of freedom.

It is worth noting that the staggering of the quasi-γ band, that could not be properly reproduced in the IBM-1 calculations, is now rather well described. This has been
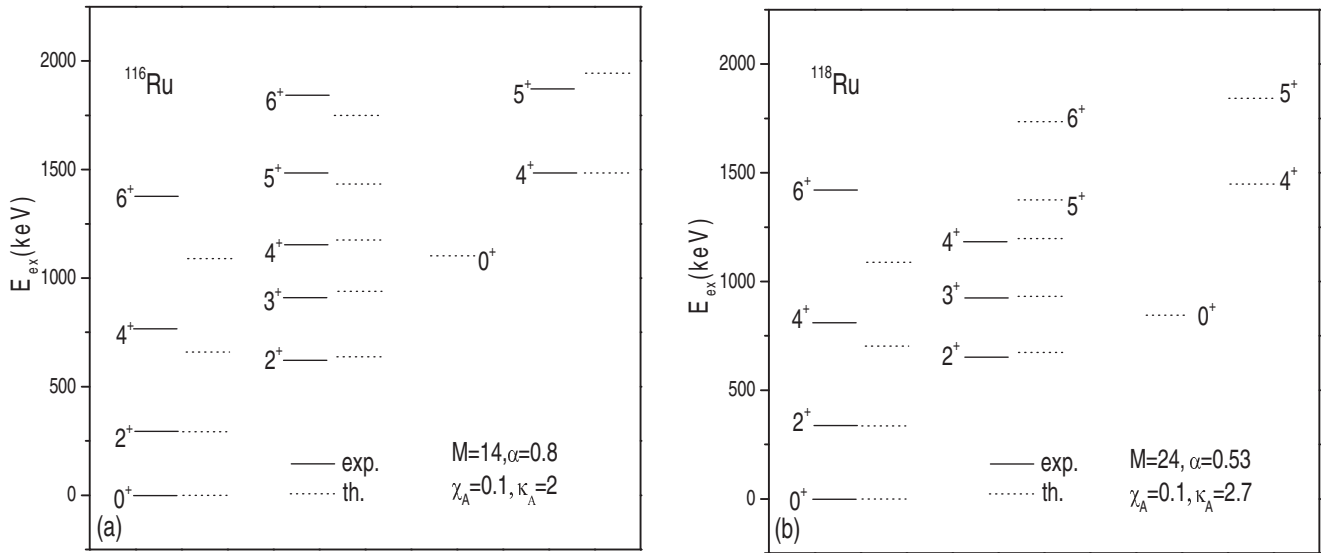
FIG. 11. Experimental excitation energies (solid lines) and excitation energies calculated using the algebraic collective model (dashed lines) for ^{116}Ru (left) and ^{118}Ru (right). The parameters used in the calculations are listed in each panel.

highlighted using the level staggering parameter, defined as

$$S(J) = \frac{E(J) - 2E(J-1) + E(J-2)}{E(2_1)}. \quad (6)$$

The experimental and the ACM calculated $S(J)$ are shown in Fig. 12. Some deviations of the theoretical values from the experimental data can be observed. These are most likely related to the softness in the γ direction of the potential energy surface. Also, theoretical candidates for 0_2^+ state around 1100 and 800 keV for ^{116}Ru and ^{118}Ru, respectively, are shown in Fig. 11. In general, these calculations show that the triaxial minimum is beginning to stabilize for ^{118}Ru. This is mainly due to the decrease of α, which is very close to the critical value of $\alpha = 0.5$, and a slight increase of κ_A. The parameters are, indeed, very close to the ones that would be expected from a transition between the O(6) limit of the IBM ($\chi_A = \kappa_A = 0$)

to the harmonic spherical vibrator limit of the Bohr model, or the U(5) limit of the IBM ($\chi_A = \kappa_A = \alpha = 0$).

V. SUMMARY

The nuclei ^{116}Ru and ^{118}Ru have been studied via γ-ray spectroscopy using the EURICA detector array, following β-decay in the WAS3ABi array. The nuclei were produced using in-flight fission of a ^{238}U beam at the RIKEN RIBF facility. Level schemes with positive-parity states up to spin $J = 6$ have been constructed. The neutron-rich isotope chain $^{108-118}$Ru has been discussed in terms of the interacting boson model and the $^{114-120}$Ru isotopes have been discussed in terms of total Routhian surfaces. The conclusions are that the very neutron-rich nuclei still show many features associated with triaxial γ-soft nuclei, represented by the O(6) symmetry, but are approaching a spherical structure, the U(5) symmetry, with increasing neutron number towards the $N = 82$ shell closure.

FIG. 12. (Color online) Energy staggering of the quasi-γ band for ^{116}Ru and ^{118}Ru.

[1] T. Sumikama, K. Yoshinaga, H. Watanabe, S. Nishimura, Y. Miyashita, K. Yamaguchi, K. Sugimoto, J. Chiba, Z. Li, H. Baba *et al.*, Phys. Rev. Lett. **106**, 202501 (2011).

[2] F. McGowan, R. Robinson, P. Stelson, and W. Milner, Nucl. Phys. A **113**, 529 (1968).

[3] N. Kaffrell, N. Trautmann, G. Herrmann, and H. Ahrens, Phys. Rev. C **8**, 320 (1973).

[4] J. Äystö, P. Jauho, Z. Janas, A. Jokinen, J. Parmonen, H. Penttilä, P. Taskinen, R. Béraud, R. Duffait, A. Emsallem *et al.*, Nucl. Phys. A **515**, 365 (1990).

[5] J. Shannon, W. Phillips, J. Durell, B. Varley, W. Urban, C. Pearson, I. Ahmad, C. Lister, L. Morss, K. Nash *et al.*, Phys. Lett. B **336**, 136 (1994).

[6] M. Bernas, S. Czajkowski, P. Armbruster, H. Geissel, P. Dessagne, C. Donzaud, H.-R. Faust, E. Hanelt, A. Heinz, M. Hesse *et al.*, Phys. Lett. B **331**, 19 (1994).

[7] F. Montes, A. Estrade, P. T. Hosmer, S. N. Liddick, P. F. Mantica, A. C. Morton, W. F. Mueller, M. Ouellette, E. Pellegrini, P. Santi *et al.*, Phys. Rev. C **73**, 035801 (2006).

[8] P. Möller, R. Bengtsson, B. Carlsson, P. Olivius, T. Ichikawa, H. Sagawa, and A. Iwamoto, At. Data Nucl. Data Tables **94**, 758 (2008).

[9] P. Möller, A. Sierk, R. Bengtsson, H. Sagawa, and T. Ichikawa, At. Data Nucl. Data Tables **98**, 149 (2012).

[10] M. Böyükata, P. Van Isacker, and I. Uluer, J. Phys. G **37**, 105102 (2010).

[11] K. Nomura, N. Shimizu, and T. Otsuka, Phys. Rev. C **81**, 044307 (2010).

[12] P. Van Isacker and G. Puddu, Nucl. Phys. **348**, 125 (1980).

[13] J. L. M. Duarte, T. Borello-Lewin, G. Maino, and L. Zuffi, Phys. Rev. C **57**, 1539 (1998).

[14] I. Stefanescu, A. Gelberg, J. Jolie, P. Van Isacker, P. von Brentano, Y. Luo, S. Zhu, J. Rasmussen, J. Hamilton, A. Ramayya *et al.*, Nucl. Phys. A **789**, 125 (2007).

[15] Y. Yano, Nucl. Instrum. Methods B **261**, 1009 (2007).

[16] T. Kubo, Nucl. Instrum. Methods B **204**, 97 (2003).

[17] Y. Mizoi, T. Kubo, H. Sakurai, K. Kusaka, K. Yoshida, and A. Yoshida, RIKEN Accelerator Progress Report No. 38, 2005 (unpublished), p. 297.

[18] S. Nishimura, H. Baba, P. Doornenbal, E. Ideguchi, T. Isobe, M. Kurata-Nishimura, Z. Li, G. Lorusso, A. Odahara, T. Nakao *et al.*, RIKEN Accelerator Progress Report No. 45, 2012 (unpublished), p. X.

[19] S. Nishimura, Prog. Theor. Exp. Phys. (2012) 03C006.

[20] S. Nishimura, Nucl. Phys. News Int. **22**, 38 (2012).

[21] P.-A. Söderström, S. Nishimura, P. Doornenbal, G. Lorusso, T. Sumikama, H. Watanabe, Z. Xu, H. Baba, F. Browne, S. Go *et al.*, Nucl. Instrum. Methods B (to be published).

[22] J. Eberth, P. V. Brentano, W. Teichert, H. Thomas, A. Werth, R. Lieder, H. Jäger, H. Kämmerling, D. Kutchin, K. Maier *et al.*, Prog. Part. Nucl. Phys. **28**, 495 (1992).

[23] M. Wilhelm, J. Eberth, G. Pascovici, E. Radermacher, H. Thomas, P. von Brentano, H. Prade, and R. Lieder, Nucl. Inst. Meth. A **381**, 462 (1996).

[24] J. Eberth, H. Thomas, P. Brentano, R. Lieder, H. Jäger, H. Kämmerfing, M. Berst, D. Gutknecht, and R. Henck, Nucl. Instrum. Methods A **369**, 135 (1996).

[25] P. Möller, B. Pfeiffer, and K.-L. Kratz, Phys. Rev. C **67**, 055802 (2003).

[26] J. Rissanen, J. Kurpeta, V.-V. Elomaa, T. Eronen, J. Hakala, A. Jokinen, I. D. Moore, P. Karvonen, A. Płochocki, L. Próchniak *et al.*, Phys. Rev. C **83**, 011301 (2011).

[27] J. C. Hardy, L. C. Carraz, B. Jonson, and P. G. Hansen, Phys. Lett. B **71**, 307 (1977).

[28] http://www.nndc.bnl.gov/ensdf/ accessed on 2013-04-01.

[29] H. Watanabe, K. Yamaguchi, A. Odahara, T. Sumikama, S. Nishimura, K. Yoshinaga, Z. Li, Y. Miyashita, K. Sato, L. Próchniak *et al.*, Phys. Lett. B **704**, 270 (2011).

[30] R. F. Casten, A. I. Namenson, W. F. Davidson, D. D. Warner, and H. G. Borner, Phys. Lett. B **76**, 280 (1978).

[31] W. Satuła, R. Wyss, and P. Magierski, Nucl. Phys. A **578**, 45 (1994).

[32] M. Brack, J. Damgaard, A. S. Jensen, H. C. Pauli, V. M. Strurinsky, and C. Y. Wong, Rev. Mod. Phys. **44**, 320 (1972).

[33] V. M. Strurinsky, Nucl. Phys. A **95**, 420 (1967).

[34] F. R. Xu, P. M. Walker, J. A. Sheikh, and R. Wyss, Phys. Lett. B **435**, 257 (1998).

[35] F. R. Xu, P. M. Walker, and R. Wyss, Phys. Rev. C **59**, 731 (1999).

[36] F. R. Xu, P. M. Walker, and R. Wyss, Phys. Rev. C **62**, 014301 (2000).

[37] F. Iachello and A. Arima, *The Interacting Boson Model* (Cambridge University Press, Cambridge, UK, 1987).

[38] R. Casten, *Nuclear Structure from a Simple Perspective*, 2nd ed. (Oxford University Press, Oxford, UK, 2000).

[39] O. Scholten, the program package PHINT, Michigan State University, 1982 (unpublished).

[40] V. Werner (private communication).

[41] A. Arima, T. Otsuka, F. Iachello, and I. Talmi, Phys. Lett. B **66**, 205 (1977).

[42] T. Otsuka, A. Arima, F. Iachello, and I. Talmi, Phys. Lett. B **76**, 139 (1978).

[43] W. Urban, M. Jentschel, R. F. Casten, J. Jolie, Ch. Bernards, B. Maerkisch, Th. Materna, P. Mutti, L. Próchniak, T. Rząca-Urban *et al.*, Phys. Rev. C **87**, 031304 (2013).

[44] D. J. Rowe, T. A. Welsh, and M. A. Caprio, Phys. Rev. C **79**, 054304 (2009).

[45] G. Thiamova, D. J. Rowe, and M. A. Caprio, Nucl. Phys. A **895**, 20 (2012).